Heliyon 10 (2024) e35846

Contents lists available at ScienceDirect

Heliyon

journal homepage: www.cell.com/heliyon

Research article

The cytoprotective effect of *Gymnema inodorum* leaf extract against hypoxia-induced cardiomyocytes injury

Sirirat Surinkaew [a,b], Dali Sun [c], Nateelak Kooltheat [a,d], Rachasak Boonhok [a,b], Voravuth Somsak [a,b], Sarawut Kumphune [e,f,*]

[a] *School of Allied Health Sciences, Walailak University, Nakhon Si Thammarat, 80160, Thailand*
[b] *Research Excellence Center for Innovation and Health Products (RECIHP), Walailak University, Nakhon Si Thammarat, 80160, Thailand*
[c] *Department of Electrical and Computer Engineering, Ritchie School of Engineering and Computer Science, University of Denver, Colorado, 80208, USA*
[d] *Hematology and Transfusion Science Research Center, School of Allied Health Sciences, Walailak University, Nakhon Si Thammarat, 80160, Thailand*
[e] *Biomedical Engineering Institute, Chiang Mai University, Chiang Mai, 50200, Thailand*
[f] *Biomedical Engineering and Innovation Research Center, Chiang Mai University, Chiang Mai, 50200, Thailand*

ARTICLE INFO

Keywords:
Gymnema inodorum
Ischemic heart disease
Hypoxia
ROS
Antioxidant
Anti-inflammatory
mRNA expression
Anti-inflammatory cytokines

ABSTRACT

Ischemic heart disease stands out as a major global contributor to mortality, with the initiation of hypoxia, marked by reduced oxygen availability, disrupting the balance of reactive oxygen species (ROS), leading to cellular injury. Exploring antioxidants derived from medicinal plants is becoming more interesting as a potential alternative treatment, especially for mitigating myocardial injury. Thus, this study aimed to assess the cytoprotective efficacy of *Gymnema inodorum* leaf extract (GIE) in a rat cardiac myoblast, H9c2, subjected to an in vitro hypoxia. The cell viability, intracellular ROS production and the expression of inflammatory cytokines were quantified, and hypoxia-induced cell morphology changes were observed using confocal fluorescence microscopy. The results showed that GIE notably enhanced cell viability, preserving membrane integrity, when compared with the hypoxic group. Remarkably, GIE significantly reduced hypoxia-induced intracellular ROS production, attributable to its inherent antioxidant properties. Furthermore, GIE significantly reduced interleukin (IL)-1β, interleukin (IL)-6 mRNA expression level and tended to reduce tumor necrosis factor-α (TNF-α) mRNA expression. In conclusion, these findings underscore the potential of GIE in mitigating hypoxia-induced myocardial injury, highlighting its robust antioxidant and anti-inflammatory attributes.

1. Introduction

Ischemic heart disease (IHD) is a cardiac condition caused by insufficient oxygen and blood supply to the heart, leading to heart attacks or acute myocardial infarctions (AMIs). As the most prevalent cardiovascular disease globally, IHD exhibits a concerning and continuous increase, ranking among the leading causes of mortality worldwide [1,2]. During myocardial ischemia, cardiac tissue undergoes hypoxia due to insufficient oxygen and metabolite supply to the at-risk area, a consequence of an occluded coronary artery. The ischemic injury triggers an imbalance in the antioxidant defense system, resulting in the overproduction of excessive reactive

* Corresponding author. Biomedical Engineering Institute (BMEI) Chiang Mai University, Chiang Mai, 50200, Thailand.
E-mail address: sarawut.kumphune@cmu.ac.th (S. Kumphune).

https://doi.org/10.1016/j.heliyon.2024.e35846
Received 9 January 2024; Received in revised form 5 August 2024; Accepted 5 August 2024
Available online 6 August 2024

oxygen species (ROS) [3]. These ROS, in turn, cause direct damage to cell membranes, instigating localized inflammation. Early inflammatory cytokines, including interleukin (IL)-1β, interleukin (IL)-6 and tumor necrosis factor-α (TNF-α), undergo upregulation in the myocardial ischemic zone, aggravating cardiomyocytes injury and death [4,5].

Studies have highlighted that even brief exposure to hypoxia induces significant cardiomyocyte apoptosis, and in vivo models show a correlation between exceptionally brief episodes of myocardial ischemia, as short as 5 mins, and the stabilization of hypoxia-inducing factor (HIF) [6,7]. Consequently, therapeutic strategies aiming to maintain ROS balance, inhibit inflammation and mitigate apoptosis emerge as promising avenues for the treatment of myocardial infarction (MI). While medicinal plants, rich in antioxidant properties, show potential in alleviating oxidative stress and preserving mitochondrial function [8,9], there remains a crucial knowledge gap regarding the specific impact of *Gymnema inodorum*'s antioxidants on cardiac hypoxia.

Gymnema inodorum (Lour.) Decne, a native plant extensively distributed across Southeast Asia and belonging to the Apocynaceae family, boasts a rich history in both cuisine and alternative medicine. Its leaves and stems have played a prominent role in various traditional practices, particularly in the Ayurvedic system, where it is widely recognized for its efficacy in diabetes treatment. Extracts of *G. inodorum*, whether in water or ethanol, showcase robust antioxidant activity, featuring polyphenols and flavonoids as active compounds [10]. Alongside its known antipyretic and anti-allergenic properties, *G. inodorum* finds applications in addressing diverse health conditions, spanning from constipation to mental symptoms, liver and stomach cancers, coronary heart disease, cataracts, rheumatoid arthritis, and gout [10–12]. Despite the well-documented benefits of *G. inodorum* for various health conditions and its recognized antioxidant properties for cellular protection and repair, a significant gap in exploration exists regarding how *G. inodorum*'s antioxidants specifically influence cardiac hypoxia. This oversight prompts the need for dedicated research to unravel the potential impact of *G. inodorum* in the context of cardiac health, especially in conditions related to oxygen deprivation such as ischemic heart disease.

This research aims to bridge the knowledge gap by investigating the in vitro cardioprotective potential of *G. inodorum* against hypoxia-induced injury in H9c2 cells. The primary hypothesis posits that the antioxidant-rich extracts of *G. inodorum* will effectively mitigate ROS imbalance, inhibit inflammation, and alleviate apoptosis. Through this research, we aspire to contribute valuable insights into *G. inodorum*'s potential role in cardiac health, laying a foundation for future therapeutic applications in the context of ischemic heart disease.

2. Materials and methods

2.1. Preparation of G. inodorum leaves extract

The first three young leaves of *G. inodorum* used in this study were collected from the Chiangda Organic Garden in Chiang Mai, Thailand, and their authenticity was confirmed by a taxonomist from Chiangmai University who deposited a voucher specimen for future studies. To extract the bioactive compounds, fresh leaves were washed, dried overnight in a hot air oven at 50 °C, and then ground into a powder using an electric blender. The powder was then mixed with distilled water at a 5 % (w/v) ratio and incubated at 60 °C with a mechanical shaker for 15 min to facilitate extraction. The supernatant was collected after centrifugation at 2500 rpm for 5 min and then lyophilized using a Beta 1–8 LSC plus freeze dryer (Martin Christ Gefriertrocknungsanlagen GmbH, Osterode am Harz, Germany) to obtain the aqueous crude extract of *G. inodorum* leaves (GIE). The percentage yield after freeze-drying was 17.43 % (w/w). The gymnemic acid concentrations was previously measured using HPLC-UV, and other potential compounds were identified using LC-QTOF/MS [13].

2.2. DPPH radical scavenging activity of GIE

To assess the in vitro free radical scavenging activity of the GI extract, a 2,2-diphenyl-2-picrylhydrazyl (DPPH) scavenging assay was performed [14]. A 10 mM DPPH solution was prepared in absolute methanol and adjusted to an optical density of 0.7 ± 0.02 at 517 nm. In a 96-well plate, 10 μl of varying concentrations, ranging from 0.063 to 6.4 mg/ml of the GIE and standard ascorbic acid were combined with 90 μl of freshly prepared DPPH reagent. The reaction mixture was incubated, avoiding exposure to the light, for 30 min at room temperature, and the optical density (O.D.) was measured at a wavelength of 517 nm using the Eon™ Microplate Spectrophotometer (BioTek Instruments, Inc., Vermont, USA). Each measurement was performed in triplicate across three individual experiments to determine the scavenging activity based on the decrease in absorbance. The percentage of DPPH radical scavenging activity was calculated using the formula: [(A_{517} of control – A_{517} of sample)/A_{517} of control] x 100. The IC_{50} value was determined from the percentage inhibition graph.

2.3. ABTS radical scavenging activity of GIE

The ABTS assay is a method used to measure the antioxidant activity of compounds, based on the decolorization of blue/green ABTS•+ by antioxidants, reducing it to ABTS• (2,2′-Azino-bis (3-ethylbenzothiazoline-6-sulfonic acid) diammonium salt. To perform this assay, 7 mM ABTS (Sigma-Aldrich) was dissolved in water, and ABTS•+ radicals were generated by mixing it with 2.45 mM potassium persulfate at a 1:1 ratio, followed by incubation and avoiding exposure to the light, for 16–18 h at room temperature. Then, the reaction mixture was diluted in absolute methanol to reach an absorbance value of 0.7 ± 0.02 at a wavelength of 734 nm. In a 96-well plate, different concentrations (0.0125–3.2 mg/ml) of standard ascorbic acid or the extracts were mixed with 90 μl of ABTS•+ working solution. The mixture was incubated for 45 min at room temperature, and absorbance was measured at 734 nm. The

percentage of ABTS•+ scavenging activity was calculated using the formula [(A_{734} of control – A_{734} of sample)/A_{734} of control] x 100, and the IC_{50} value was derived from the percentage inhibition graph.

2.4. Cell culture

The H9c2 rat cardiomyoblast cell line (ATCC® CRL-1446) was cultured in Dulbecco's Modified Eagle Medium (DMEM) supplemented with 10 % fetal bovine serum (FBS) and 1 % penicillin/streptomycin (Thermo Fisher Scientific). The medium was changed every 2 days, and the cells were maintained at 37 °C in a humidified atmosphere containing 5 % CO_2/95%-humidified air. Cells were grown until they reached approximately 80 % confluent, after which they were trypsinized with 0.05 % trypsin for further experiments.

2.5. Induction of in vitro hypoxia

The H9c2 cells were seeded in 12-well plates at a density of 1×10^5 cells/well. The cells were cultured in complete DMEM and maintained at 37 °C in a humidified atmosphere containing 5 % CO_2 for 48 h. Hypoxic conditions were induced by replacing the media with 1.5 ml of serum-free DMEM before overlaying mineral oil (1.5 ml) on the culture media. To measure the O_2 remaining in the culture media under hypoxic conditions, the cells were exposed to hypoxia for 1, 2, 4, 6, 12, 18, 24, 36, 48 or 72 h. After each exposure, the culture media was collected using a syringe, and the O_2 partial pressure (PO_2) was measured at the spot using the OPTI CCA-TS2 Blood Gas and Electrolyte Analyzer (OPTIMedical, GA, USA). The O_2 saturation obtained in each time point was normalized with the control group (normoxia).

2.6. Cell viability

The H9c2 cells were seeded at a density of 5×10^3 cells per well in 96-well plates containing complete Dulbecco's Modified Eagle Medium and were incubated in 5 % CO_2/95%-humidified air atmosphere at 37 °C for 48 h. The cytotoxicity of GIE was evaluated using H9c2 cells. Cells were exposed to 20 concentrations of GIE, in a logarithmic scale, ranging from 1 to 10,000 μg/ml, for a duration of 24 h at 37 °C. Following treatment, cell viability was assessed by replacing culture media with MTT solution (3-(4,5-dimethyl-2-thiazolyl)-2,5-diphenyl-2-H-tetrazolium bromide, 0.5 mg/ml in phosphate-buffered saline) and incubated in the dark for 4 h at 37 °C. The formazan crystal was dissolved with dimethyl sulfoxide (DMSO), and then measured for optical density (O.D.) at a wavelength of 570 nm using a microplate spectrophotometer (Eon™ Microplate Spectrophotometer, BioTek Instruments, Inc., VT, USA). The cytotoxicity of GIE was then analyzed by curve fitting, and the 50 % cytotoxicity concentrations (CC50), 10 % cytotoxicity concentrations (CC10) and 5 % cytotoxicity concentrations (CC5) were calculated. The concentration lower than CC10 was then used for further experiments.

To determine the protective effect of GIE under hypoxia condition, the cells were pretreated with GIE at concentrations of 10, 20 and 40 μg/ml for 18 h. At the end of the pretreatment procedure, the hypoxic condition was induced for 4 h, as described previously [15,16], along with GIE. Cell viability was subsequently assessed using the MTT test, and the relative percentage of cell viability was compared with that of the control group.

2.7. Determination of intracellular ROS production

Cells were seeded in a black-walled 96-well plate at a density of 5×10^3 cells/well and incubated overnight in complete DMEM at 37 °C with 5 % CO_2 and 95 % humidified air. After incubation, the medium containing 25 μM 2′,7′-dichlorofluorescin diacetate (DCFH-DA, Sigma-Aldrich) was added to the reaction. Induction of hypoxic condition was performed by overlaying the culture well with mineral oil for 4 h. Intracellular ROS production was measured by fluorescence intensity, using excitation and emission wavelengths of 498 and 522 nm, respectively, with the Synergy Mx Microplate Reader (BioTek Instruments, Inc., VT, USA).

2.8. Fluorescence imaging

The H9c2 cells were cultured on sterile coverslips placed in a 6-well plate at a density of 2×10^5 cells/well. They were maintained in complete DMEM (2000 μl/well) overnight at 37 °C in a 5 % CO_2 incubator. Then, cells were pre-treated with 10 μg/ml GIE for 18 h before being subjected to 4 h of hypoxia. At the end of hypoxic condition, cells were washed twice with PBS and fixed with 2 % paraformaldehyde and 0.05 % glutaraldehyde and incubated at room temperature for 30 min. The cells were then stained with 500 μl of PI/RNase staining solution (Cell Signaling Technology, Inc., MA, USA) and incubated in the dark at room temperature for 15 min. Cells were again washed twice with PBS. Next, a few drops of Neo-mount anhydrous mounting medium (Engelbrecht GmbH, Germany) were added to a new glass slide. The stained cells on the coverslip were placed on the glass slide and kept in the dark, moist chamber. The stained cells were observed under a Confocal Laser Scanning Microscope (Leica SP 5 II, Germany).

2.9. RNA extraction and quantitative reverse transcription polymerase chain reaction (qRT-PCR)

Determining the effect of GIE on the inflammatory cytokine mRNA expression, GENEzol™ Reagent (Geneaid, Taiwan) was added directly to the culture well containing 7×10^4 cultured cells for cell lysis. Total RNA was then extracted using a GF-1 extraction kit (Vivantis Technologies, Malaysia). The quantity and quality of extracted RNA was measured using NanoDrop One© (Thermo Fisher

Scientific, Massachusetts, USA). Conversion of mRNA to complementary DNA was performed using 0.6 μg of RNA template according to the manufacturer's protocol for the Viva cDNA Synthesis Kit (Vivantis Technologies, Selangor, Malaysia). The quantitative PCR (qPCR) reaction mix was prepared using iTaq™ Universal SYBR® Green Supermix kit (Bio-Rad Laboratories, California, USA). Ten microliters of iTaq™ Universal SYBR Green Supermix (2X) was combined with 300 ng of cDNA and 1 μl each of 200 mM forward and reverse primers. The final volume of the reaction mix was adjusted to 20 μl using diethyl pyrocarbonate (DEPC) water. SYBR Green primers were IL-1β (Forward primer: 5′ CACCTCTCAAGCAGAGCACAG; Reverse primer: 5′ GGGTTCCATGGTGAAGTCAAC), IL-6 (Forward primer: 5′ TCCTACCCCAACTTCCAATGCTC; Reverse primer: 5′ TTGGATGGTCTTGGTCCTTAGCC) [17] and TNF-α (Forward primer: 5′ CACGCTCTTCTGTCTACTGA; Reverse primer: 5′ GGACTCCGTGATGTCTAAGT) [18].

The relative gene expression levels were calculated from triplicate samples, normalizing with the expression of house keeping gene, Glyceraldehyde-3-phosphate dehydrogenase (GAPDH) (Forward primer: 5′ TTCCTACCCCCAATGTATCCG; Reverse primer: 5′ CATGAGGTCCACCACCCTGTT) [19], and HPRT (Forward primer: 5′ CTCATGGACTGATTATGGACAGGAC; Reverse primer: 5' GCAGGTCAGCAAAGAACTTATAGCC) [17]. The StepOnePlus™ Real-Time PCR system software (Applied Biosystems, Waltham, Massachusetts, USA) was programmed with a thermal cycle at 95 °C for 30 s, followed by 40 cycles at 60 °C for 30 s and 72 °C for 60 s for IL-1β, IL-6, GAPDH, HPRT and ACTB. For TNF-α, the cycle parameters were 95 °C for 15 s and 56 °C for 60 s over 40 cycles. Relative fold changes in gene expression were determined using the $2^{-\Delta\Delta Ct}$ method.

2.10. Statistical analysis

All data are expressed in mean ± SEM. Statistical comparisons were conducted using one-way ANOVA, followed by either Dunnett's multiple comparison test or Tukey's multiple comparison test for comparison between each time point and the control. Paired Student's t-tests were used for comparing two groups of studies. The software GraphPad Prism (Version 9.0) was used for all statistical analyses. A p-value less than 0.05 was considered to be statistically significant.

3. Results

3.1. Radical scavenging activity of GIE

The scavenging activity of DPPH and $ABTS^{+}$ radicals was observed for their potential antioxidant properties. The DPPH scavenging activity of GIE was 15 ± 2.6 % at 0.4 mg/ml, whereas ascorbic acid, used as the standard antioxidant, exhibited a maximum scavenging activity of 95 ± 1.8 % at the same concentration (Fig. 1a, see also Supplementary Data 1). The scavenging ability of GIE was further assessed using the ABTS assay, showing 19 ± 4.0 % scavenging activity at 0.4 mg/ml. In comparison, ascorbic acid demonstrated 100 ± 0.1 % scavenging activity at 0.4 mg/ml (Fig. 1b–Supplementary Data 1).

3.2. Effect of GIE on cytotoxicity

The cytotoxicity of GIE was evaluated using H9c2 cells exposed to 20 different concentrations of GIE, ranging from 1 to 10,000 μg/ml, for 24 h at 37 °C. Cell viability was measured using the MTT assay, and the cytotoxicity percentages were normalized against a control group that was not treated with GIE. Further analysis involved curve fitting, providing insights into the cytotoxicity concentrations of GIE. This analysis, illustrated in Fig. 2, showed the correlation between cell viability percentage and cytotoxicity. The results revealed key concentrations: the median cytotoxicity concentration (CC50) of GIE was determined to be 1,096.48 μg/ml, while the concentrations causing 10 % cytotoxicity (CC10) and 5 % cytotoxicity (CC5) were found to be 61.29 μg/ml and 22.98 μg/ml,

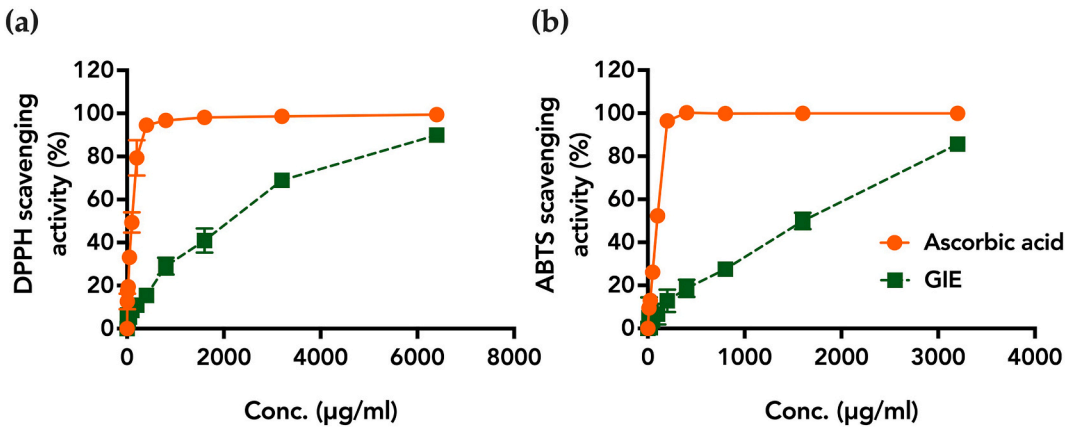

Fig. 1. Scavenging activities of *Gymnema inodorum* extract (GIE) by DPPH and ABTS assay. The scavenging activities of GIE concentrations were performed by DPPH (a) and ABTS (b) assay, ranging from 0 to 6.4 mg/ml and 0–3.2 mg/ml, respectively. Each experiment was performed in triplicate with a minimum of 3 independent experiments.

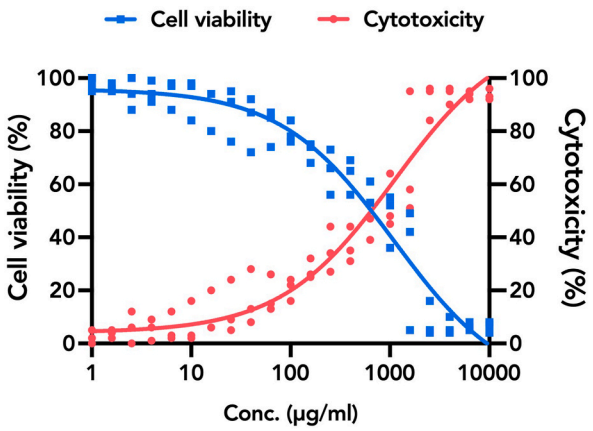

Fig. 2. Cytotoxicity effect of *Gymnema inodorum* extract (GIE) varying from 1 to 10,000 µg/ml. The cytotoxic activity of GIE on H9c2 was performed after incubation at 37 °C for 24 h. Each dot represents the cytotoxic effect of GIE at different concentrations. The graph depicts the correlation between cytotoxicity (on the right y-axis) and cell viability (on the left y-axis). Each concentration was measured in triplicate with a minimum of 3 independent experiments.

respectively (see also Supplementary Data 2). Following this analysis, the concentration inducing a 10 % decrease in cell viability (CC10) or ensuring 90 % cell survival was selected for subsequent experiments, ensuring optimal conditions for further investigation.

3.3. GIE restores cardiac cell viability induced by hypoxia

To determine the effective period for inducing hypoxia, H9c2 cells were exposed to hypoxia at different time intervals. The culture media were collected and the PO_2 level was measured. In control group (normoxia), the O_2 concentration in culture media was 147 ± 1.2 mmHg, then the percentage of O_2 saturation in each time point was compared with control group (see also Supplementary Data 3). The results showed that the O_2 level in culture media was significantly reduced after 4 h of hypoxia to 93.1 ± 0.90 % and gradually reduced to 91.6 ± 1.03 %, 87.1 ± 0.93 %, 86.6 ± 0.07 %, 84.2 ± 0.24 %, 80.9 ± 0.74 %, 79.5 ± 0.76 % and 72.0 ± 4.80 % at 6, 12, 18, 24, 36, 48 and 72 h, respectively, compared with control group (Fig. 3). Therefore, the 4-hr period of hypoxia was chosen for use as the hypoxia model in further experiments.

The effect of GIE under hypoxia condition was also determined. H9c2 cells were pretreated with GIE at the concentrations of 10, 20 or 40 µg/ml for 24 h before and during the 4-hr period of hypoxia. Cell viability was measured by MTT assay. Hypoxia condition significantly reduced the percentage of cell viability to 48.9 ± 3.74 %, compared with control. Pretreatment with GIE at any concentrations, 10, 20 or 40 µg/ml, significantly increased cell viability to 72.9 ± 3.69 %, 75.7 ± 5.02 % and 77.3 ± 5.03 %, respectively, compared with the hypoxic group (Fig. 4a), indicating GIE's protective effect against hypoxia-induced cell death. However, there was no significant difference observed among the different GIE-treated groups.

To visualize the physiological effects of GIE under hypoxia condition, hypoxia induced morphology change was observed under

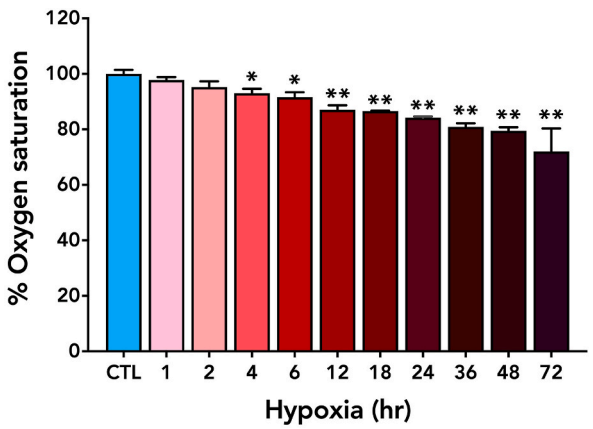

Fig. 3. Oxygen saturation percentage in H9c2 culture media subjected to hypoxia from 1 to 72 h. The percentage of oxygen saturation in H9c2 culture media was monitored over a period of 1–72 h under hypoxic conditions. The remaining oxygen partial pressure (PO_2) in the culture media was measured and normalized against the control group (CTL, normoxia). Statistical significance was determined using Dunnett's multiple comparison test, with * $p < 0.05$ and **$p < 0.0001$ vs. CTL. Each experimental condition was performed with a sample size of $n = 3$.

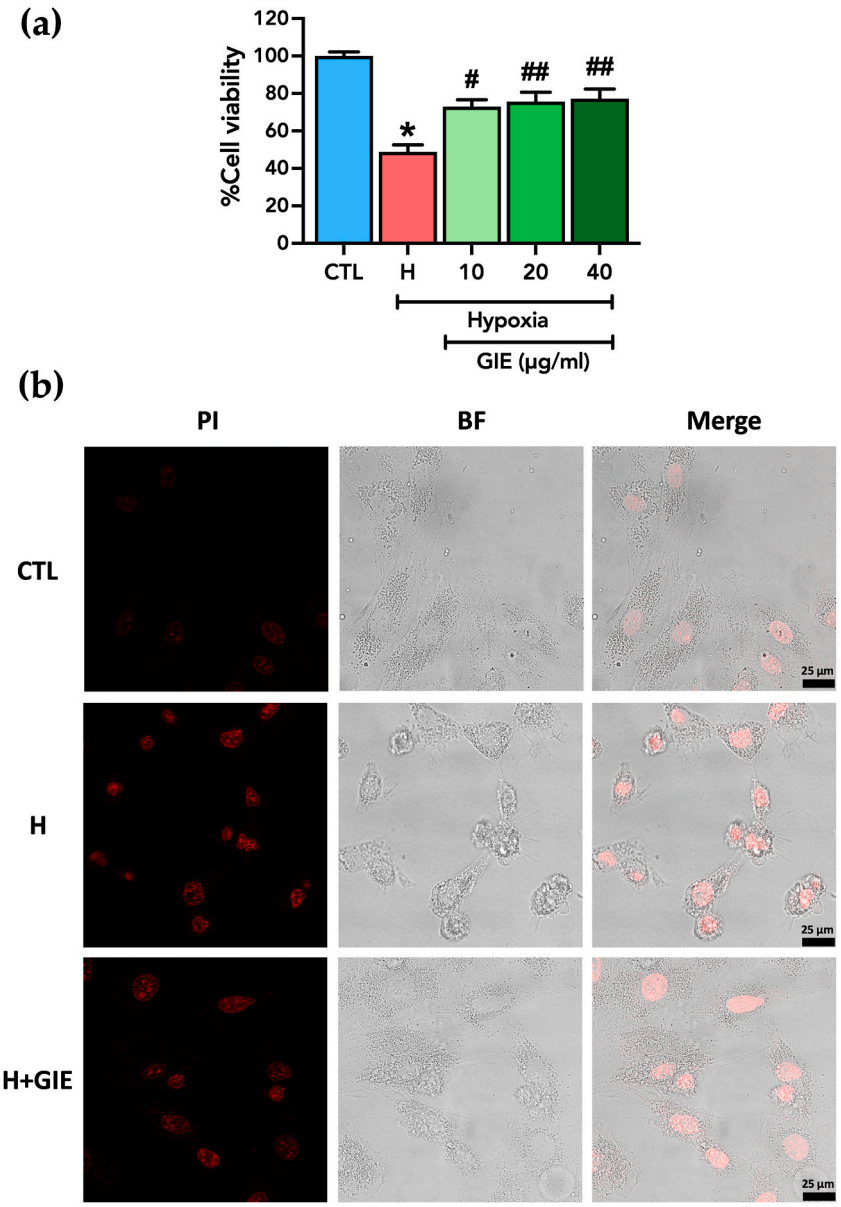

Fig. 4. Effect of *Gymnema inodorum* extract (GIE) on hypoxia-induced cell death: a) Cell viability was measured by MTT assay after exposure to hypoxia for 4 h, compared with GIE treated groups at concentrations of 10, 20 and 40 μg/ml. Statistical significance was determined using Tukey's multiple comparison test, with * $p < 0.0001$ vs. control (CTL, normoxia) and #$p < 0.01$ vs. hypoxia (H). Each experiment was performed in triplicate with a minimum of 3 independent experiments. b) Qualitative analysis of cell apoptosis was conducted in the control group (CTL), hypoxia group (H) and GIE-treated group. GIE at a concentration of 10 μg/ml was administered before and during hypoxia, followed by observation using confocal microscope with propidium iodide (PI) staining. Images illustrate PI staining, bright field (BF), and merged images. Scale bar represents 25 μm.

confocal microscope, stained with PI. Hypoxia caused significant apoptosis in H9c2 cells, as shown by condensed nuclei and disruption in membrane integrity. Remarkably, in the GIE-treated group, H9c2 nuclei reverted to their normal morphology (Fig. 4b, see also Supplementary Data 4).

3.4. Treatment of GIE before and during hypoxia reduces ROS production

To detect the level of reactive oxygen species (ROS) generation after treatment with GIE, DCFH-DA was used as a fluorescent probe. Under the 4-hr period of hypoxia, it was observed that relative ROS production increased 2.9-fold, compared with control. Treatment with GIE before and during hypoxia at any concentration, 10, 20 or 40 μg/ml, significantly reduced ROS production, in dose dependent

manner, to 1.7 ± 0.32, 2.2 ± 0.41 and 2.4 ± 0.49-fold, respectively, compared with hypoxic group (Fig. 5a). The fluorescence images of DCF were also captured using a confocal microscope. H9c2 cells exposed to hypoxia demonstrated a notable change in morphology. The fluorescence intensity was detected mostly in cytoplasm. The cytological effect was attenuated in the GIE-treated group, observed by reverse cell morphology, which demonstrated reduced DCF fluorescence intensity (Fig. 5b, see also Supplementary Data 5). Confocal microscopy confirmed that GIE mitigated hypoxia-induced morphological changes and ROS accumulation.

3.5. Inflammatory responses and anti-inflammatory effects of GIE in hypoxic H9c2 cells

The inflammatory responses of H9c2 cells under hypoxia were examined by quantifying the mRNA expression of proinflammatory cytokines IL-1β, IL-6 and TNF-α mRNA using quantitative real-time PCR (Fig. 6). The anti-inflammatory effects of GIE were assessed at

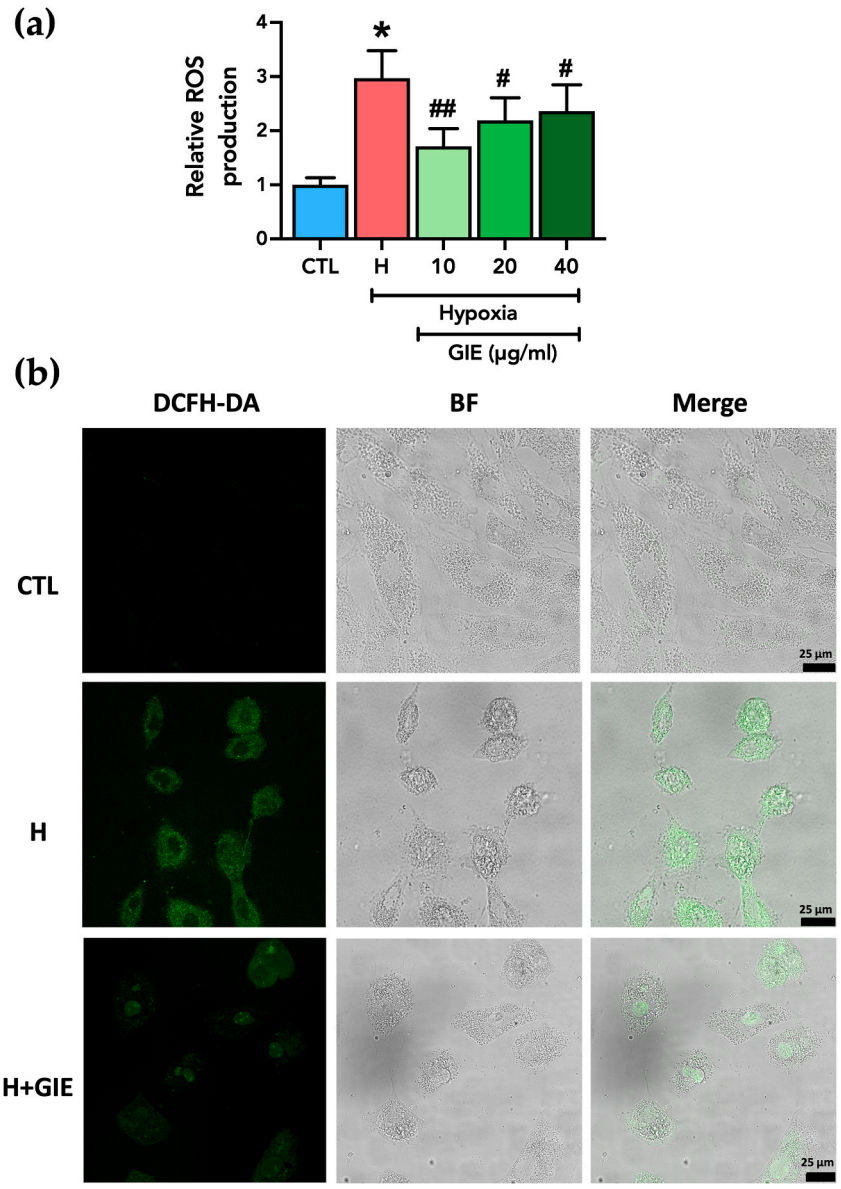

Fig. 5. Effect of *Gymnema inodorum* extract (GIE) on intracellular ROS production under hypoxia conditions: a) Fluorescence intensity representing relative ROS production was determined in the hypoxia group and compared with GIE-treatment groups. Statistical significance was assessed using Tukey's multiple comparison test, with * $p < 0.05$ vs. control (CTL, normoxia) and #$p < 0.01$ and ##$p < 0.05$ vs. hypoxia (H) using paired *t*-test. Each experiment was performed in triplicate with a minimum of 3 independent experiments. b) Analysis of ROS formation using DCFH-DA staining by confocal microscope was performed on H9c2 cells in the control group (CTL), hypoxia group (H) and GIE-treated group. Morphology changes of H9c2 cells under hypoxia and pretreatment with GIE at 10 µg/ml was illustrated. Images show DCFH-DA staining, bright field (BF), and merged images. Scale bar represents 25 µm.

concentrations of 10, 20 and 40 μg/ml and presented as relative fold-changes compared with the control (normoxia). H9c2 cells subjected to hypoxic conditions exhibited a significant upregulation of IL-1β mRNA by 1.5 ± 0.06-fold compared with the control. Treatment with GIE at any concentration (10, 20 or 40 μg/ml), administered before and during hypoxia, significantly reduced IL-1β mRNA expression to 0.9 ± 0.09, 0.8 ± 0.11 and 0.9 ± 0.04-fold, respectively, compared with the hypoxia group (Fig. 6a). There were no significant differences in IL-1β mRNA expression levels between the different GIE-treated groups. These results suggest that GIE effectively downregulates IL-1β mRNA expression under hypoxic conditions, highlighting its potential therapeutic implications. However, a 4-h period of hypoxia did not significantly alter the mRNA expression levels of IL-6 and TNF-α compared with the control (Fig. 6b–c). This indicates that the anti-inflammatory effects of GIE in the context of hypoxia may be specific to IL-1β modulation.

4. Discussion

In ischemic heart disease, arterial stenosis hinders blood supply to the myocardium, leading to myocardial infarction (MI). Subsequently, insufficient oxygen delivery to organs and heart tissues results in hypoxia [20]. Under these conditions, there is an escalation in reactive oxygen species (ROS), contributing to myocardial apoptosis. This study elucidates the scavenging activities of *Gymnema inodorum* extract (GIE) in hypoxia-induced cardiac injury using an in vitro model. The effects of GIE are manifested through the reduction of ROS production, attenuation of proinflammatory cytokine IL-1β expression, and augmentation of cell viability against hypoxia-induced injury. Furthermore, the cardioprotective efficacy of GIE is affirmed by confocal microscopy, revealing that pretreatment with GIE preserves cellular integrity and prevents cellular apoptosis under hypoxic conditions.

For the first time, this study has shown the cytotoxicity of water extract of GIE on cardiomyoblasts, revealing its safe concentration range for further experimentation. The median cytotoxicity concentration (CC50) of GIE, CC10 and CC5 were determined to be 1,096.48, 61.29 and 22.98 μg/ml, respectively (Fig. 2). These findings align with previous studies, confirming the safety profile of Gymnema species. A study on RAW264.7 macrophages demonstrated that GIE exhibited minimal cytotoxicity at concentrations up to 400 μg/ml [21], highlighting its potential to mitigate oxidative damage and inflammation. This supports our results of GIE's protective effects and low cytotoxicity in cardiac cells. Additionally, research on *Gymnema sylvestre*, another Gymnema species, showed a CC50 of 164.9 ± 1.0 μg/ml in a pancreatic β-cell line [22], approximately seven times lower than our findings in cardiomyoblasts. This suggests that cardiomyocytes are more resistant to phytochemicals. However, we selected the CC10 concentration to ensure 90 % cell viability, providing optimal conditions for assessing GIE's protective effects under hypoxic conditions.

The antioxidant activities of the water extract of *G. inodorum* leaf (GIE) through DPPH (2,2-diphenyl-1-picrylhydrazyl) and ABTS free radical scavenging assays were determined. The results revealed the scavenging activity of GIE, confirming its potential as an antioxidant. GIE's composition include gymnemic acid, polyphenols, flavonoids, vitamin E, vitamin C, carotenoids, quinic acids, phenolics, quercetin, kaempferol and triterpenoid saponins, which contribute to its robust antioxidant properties [12,13,23,24]. Among these, *G. inodorum* exhibits its highest antioxidant activities through vitamin C, vitamin E, carotenoids, tannins, and total phenolics, with vitamin E being notably abundant [12]. These antioxidants play a pivotal role in safeguarding against disorders induced by oxidant damage. They function by either delaying or inhibiting the oxidation of lipids or other molecules, thereby impeding the initiation or propagation of oxidative chain reactions [25]. Additionally, they help prevent or repair cellular damage inflicted by oxygen [12]. Furthermore, *G. inodorum* belongs to the same family as *G. sylvestre*, a plant renowned for its significant pharmacological activities, encompassing antioxidant, antibiotic, anti-inflammatory, antiviral, gastro- and hepatoprotective, anticancer, and lipid-lowering properties [26]. Our findings underscore the notable efficacy of GIE in scavenging free radicals, positioning it as a promising natural extract-based cardioprotective agent for therapeutic interventions against myocardial injury related to ischemic heart disease.

To determine the optimal time point for inducing hypoxia, H9c2 cells were exposed to hypoxic conditions over varying durations. Our results revealed that a 4-hr hypoxia induction, overlaid with mineral oil, was the minimum period that significantly reduced the O_2

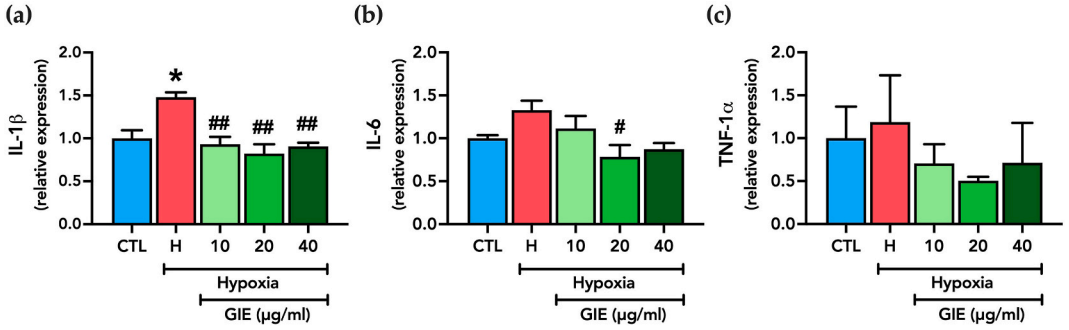

Fig. 6. Anti-inflammatory activities of *Gymnema inodorum* extract (GIE) in response to hypoxia. The relative expression of inflammatory cytokines was assessed in the control group (CTL), hypoxia group (H) and GIE-treated groups; a) GIE attenuated IL-1β mRNA expression; b) Quantitative analysis of IL-6 mRNA expression and c) Quantitative analysis of TNF-1α mRNA expression. Statistical significance was determined using Tukey's multiple comparison test, with * $p < 0.05$ vs. CTL, #$p < 0.05$ and ##$p < 0.01$, vs. hypoxia (H). Each experimental condition was performed with a sample size of $n = 3$ per group.

levels in the culture media (Fig. 3). Consequently, a 4-hr hypoxia induction was chosen to evaluate the protective effects of GIE. Under normoxic conditions, the O_2 concentration in the cell culture incubator is 18.6 % of 760 mmHg, equivalent to 141 mmHg [27]. The initiation of hypoxic exposure is generally considered the moment when the doors of the hypoxic incubator are sealed, a process that may extend from several minutes to several hours. Importantly, there is no specific threshold of PO_2; any decrease in PO_2 that significantly causes biological modifications can be termed hypoxia. Previous studies have indicated that even brief hypoxic periods, such as 2 h, can markedly activate AMPK to P-AMPK [28]. This activation serves as the central mediator of the cellular response to energetic stress and maintains mitochondrial homeostasis [28–31]. In this study, we replicated the acute hypoxia model by overlaying mineral oil on cell culture media with depleted serum. After 4-hr interval, the O_2 sensor detected a gradual reduction in the O_2 saturation level within the cell culture media [27]. Throughout this period, mitochondria, recognized as principal oxygen consumers and primary contributors to ROS production, played a crucial role in preserving other mitochondrial functions and maintaining cellular metabolism. Hypoxia triggered alterations in mitochondrial morphology, metabolism, protein composition of the electron transport chain, and the rate of respiration [32]. These adaptations are essential for maintaining the integrity of mitochondrial membranes under low oxygen conditions and regulating ROS production levels. However, substantial evidence suggests that mitochondria often struggle to adapt to the hypoxic environment [4,33]. Hypoxia induces reductive carboxylation, a process shown to escalate ROS production, disrupt cellular regulation through various pathways, compromise mitochondrial membrane potential, and ultimately lead to cardiomyocyte apoptosis [34–36].

Hypoxia-inducible factor (HIF) is a crucial regulator in cellular responses to hypoxia, presenting six distinct types: HIF-1α, HIF-1β, HIF-2α, HIF-2β, HIF-3α, and HIF-3β [37]. Among these, HIF-1α holds prominence for being the most abundantly expressed and plays a pivotal role in inflammatory processes in the heart and other organs during hypoxia [38,39]. Within the first minutes of hypoxia incubations, the activity of prolyl hydroxylases (PHDs) are inhibited by the lack of oxygen and metabolites from TCA cycle, such as fumarate and succinate [40–42]. Additionally, the generation of mitochondrial reactive oxygen species (ROS) may further impede PHD activity [43]. Consequently, the inactivation of PHDs allows stabilization of HIF-1α, enabling its dimerization with the HIF-1β subunit and subsequent translocation to the nucleus. HIF, in turn, orchestrates the regulation of multiple genes integral to maintaining oxygen homeostasis, steering cell survival and differentiation, and actively participating in cardiac metabolism and development [44]. Previous studies have indicated that HIF-1α can bind to approximately 400 target genes, promoting transcription with implications for cellular responses [39,45]. HIF-1α also play a crucial role in orchestration angiogenic processes within hypoxic regions, primarily through the regulation of vascular endothelial growth factor (VEGF). This regulatory mechanism is pivotal for tissue repair during myocardial infarction, fostering cell division, angiogenesis and the formation of new blood vessels to enhance cell proliferation and repair damaged tissue [46]. Furthermore, increased expression of HIF-1α contributes to the stimulation of macrophage migration and secretion, influencing the release of pro-inflammatory cytokines and growth factors in response to inflammation at the target tissue [39,47].

Numerous pro-inflammatory cytokines, including interleukin-6 (IL-6), tumor necrosis factor-alpha (TNF-α), and the interleukin-1 (IL-1) family, have been associated with various cardiovascular diseases (CVDs), which are increasingly recognized as conditions characterized by an adverse pro-inflammatory state [48]. In the present study, IL-1β, IL-6 and TNF-α were selected for analysis due to their critical roles in the inflammatory response following cardiac injury, particularly hypoxia/reoxygenation injury. These proinflammatory cytokines are predominantly produced by cardiomyocytes and are central to the inflammatory reactions and subsequent damage in cardiac tissues. IL-1β is a potent mediator of the acute inflammatory response, contributing to the upregulation of adhesion molecules and the recruitment of leukocytes to the site of injury [49]. IL-6 is another key cytokine produced by cardiomyocytes in response to stress, playing a significant role in mediating inflammation [50]. TNF-α is a major proinflammatory cytokine that exacerbates inflammation, promotes apoptosis, and contributes to adverse remodeling in cardiac tissues following injury [51]. These cytokines were selected because they are directly involved in the pathophysiology of hypoxia-induced cardiac injury and are therefore relevant targets for evaluating the anti-inflammatory effects of GIE. Among these, IL-1β emerges as an early proinflammatory cytokine, with its initial surge potentially contributing to the catastrophic events of acute ischemic diseases [52]. In line with these observations, the present study highlights a significant increase in the expression of the pro-inflammatory cytokine IL-1β under hypoxic conditions, contrasting with no significant changes in IL-6 and TNF-α level. The noteworthy elevation of IL-1β is particularly significant, implicating its role in the development of cardiovascular disease [53]. The results demonstrated that GIE effectively mitigates cellular oxidative damage by scavenging intracellular ROS and reducing the production of inflammatory cytokine IL-1β. Notably, it prevented cellular apoptosis observed by confocal imaging. This protective effect aligns with recent research indicating that GIE may activate the antioxidant gene SOD_2. This activation influences the inflammation process by regulating ROS levels, ultimately suppressing the expression of the proinflammatory cytokine genes TNF-α and IL-6 [21]. Furthermore, the cardioprotective effect of GIE were evidence in a recent study, showcasing its ability to enhance cardiac function during malaria infection in mice [54]. This finding suggests that early-stage treatment targeting IL-1β may hold therapeutic potential in managing cardiovascular disease.

5. Conclusion

In conclusion, our findings highlight the notable efficacy of *Gymnema inodorum* leaf extract (GIE) in alleviating hypoxia-induced myocardial injury by reducing intracellular ROS generation and attenuating the production of pro-inflammatory cytokines. These results position GIE as a promising natural cardioprotective agent for therapeutic interventions against ischemic heart disease-related myocardial injury. Further comprehensive investigations into its cardioprotective mechanisms, as well as pre-clinical studies in in vivo models, are necessary to explore its potential therapeutic applications.

Funding

This study was funded by the Research Institute for Health Sciences, Walailak University [grant number 2020–2022], and Chiang Mai University through Biomedical Engineering and Innovation Research Center, Chiang Mai University [grant number 2023].

Data availability statement

The data that support the findings of this study are included within the paper and in the Supplementary Data section. For additional data, interested individuals may request access from the corresponding author.

CRediT authorship contribution statement

Sirirat Surinkaew: Writing – original draft, Software, Methodology, Investigation, Funding acquisition, Formal analysis, Data curation, Conceptualization. **Dali Sun:** Writing – review & editing. **Nateelak Kooltheat:** Methodology, Formal analysis. **Rachasak Boonhok:** Methodology. **Voravuth Somsak:** Methodology. **Sarawut Kumphune:** Writing – review & editing, Supervision, Funding acquisition, Conceptualization.

Declaration of competing interest

The authors declare that they have no known competing financial interests or personal relationships that could have appeared to influence the work reported in this paper.

Acknowledgements

The authors gratefully acknowledge the Research Institute for Health Sciences at Walailak University for their support with laboratory facilities. Special thanks are extended to Dr. Sakaewan Ounjaijean from the School of Health Science Research at the Research Institute for Health Sciences, Chiang Mai University, for providing the *Gymnema inodorum* leaf extract used in this research.

Appendix A. Supplementary data

Supplementary data to this article can be found online at https://doi.org/10.1016/j.heliyon.2024.e35846.

References

[1] C.N.C.f.H. Statistics, Leading causes of death, Available from: https://www.cdc.gov/nchs/fastats/leading-causes-of-death.htm#print, 2024 May 2, 2024.
[2] M.A. Khan, et al., Global epidemiology of ischemic heart disease: results from the global burden of disease study, Cureus 12 (7) (2020) e9349.
[3] N. Patil, V. Chavan, N.D. Karnik, Antioxidant status in patients with acute myocardial infarction, Indian J. Clin. Biochem. : Indian J. Clin. Biochem. 22 (1) (2007) 45–51.
[4] J. Zhang, et al., Overexpression of exosomal cardioprotective miRNAs mitigates hypoxia-induced H9c2 cells apoptosis, Int. J. Mol. Sci. 18 (4) (2017).
[5] Q. He, et al., Lycopene attenuates inflammation and apoptosis in post-myocardial infarction remodeling by inhibiting the nuclear factor-κB signaling pathway, Mol. Med. Rep. 11 (1) (2015) 374–378.
[6] T. Eckle, et al., Hypoxia-inducible factor-1 is central to cardioprotection: a new paradigm for ischemic preconditioning, Circulation 118 (2) (2008) 166–175.
[7] R. Zhao, et al., Inhibition of long noncoding RNA BDNF-AS rescues cell death and apoptosis in hypoxia/reoxygenation damaged murine cardiomyocyte, Biochimie 138 (2017) 43–49.
[8] H. Yu, et al., Gypenosides alleviate myocardial ischemia-reperfusion injury via attenuation of oxidative stress and preservation of mitochondrial function in rat heart, Cell Stress Chaperones 21 (3) (2016) 429–437.
[9] A. Shaito, et al., Herbal medicine for cardiovascular diseases: efficacy, mechanisms, and safety, Front. Pharmacol. 11 (2020), 422-422.
[10] J.P. An, et al., Oleanane triterpenoids from the leaves of Gymnema inodorum and their insulin mimetic activities, J. Nat. Prod. 83 (4) (2020) 1265–1274.
[11] P. Sukum, et al., Determination of elements in Gymnema inodorum lour by particle induced X-ray emission (PIXE), Biol. Trace Elem. Res. 192 (2) (2019) 330–335.
[12] A. Chanwitheesuk, A. Teerawutgulrag, N. Rakariyatham, Screening of antioxidant activity and antioxidant compounds of some edible plants of Thailand, Food Chem. 92 (3) (2005) 491–497.
[13] N. Jeytawan, et al., Antioxidant and phytochemical potential of and phytochemicals in Gymnema inodorum (lour.) Decne in northern Thailand, Plants 11 (24) (2022).
[14] M. Chatatikun, A. Chiabchalard, Thai plants with high antioxidant levels, free radical scavenging activity, anti-tyrosinase and anti-collagenase activity, BMC Complement Altern Med 17 (1) (2017) 487.
[15] K. Kongpol, et al., Endothelial-cell-derived human secretory leukocyte protease inhibitor (SLPI) protects cardiomyocytes against ischemia/reperfusion injury, Biomolecules 9 (11) (2019) 678.
[16] H. Strijdom, et al., Nitric oxide production is higher in rat cardiac microvessel endothelial cells than ventricular cardiomyocytes in baseline and hypoxic conditions: a comparative study, Faseb. J. 20 (2) (2006) 314–316.
[17] A. Peinnequin, et al., Rat pro-inflammatory cytokine and cytokine related mRNA quantification by real-time polymerase chain reaction using SYBR green, BMC Immunol. 5 (2004) 3.
[18] Y. Paz, et al., Effect of tumor necrosis factor-alpha on endothelial and inducible nitric oxide synthase messenger ribonucleic acid expression and nitric oxide synthesis in ischemic and nonischemic isolated rat heart, J. Am. Coll. Cardiol. 42 (7) (2003) 1299–1305.
[19] J. Pu, et al., Propofol alleviates apoptosis Induced by chronic high glucose Exposure via Regulation of HIF-1α in H9c2 cells, Oxid. Med. Cell. Longev. (2019) 4824035, 2019.

[20] P. Severino, et al., Ischemic heart disease pathophysiology paradigms overview: from plaque activation to microvascular dysfunction, Int. J. Mol. Sci. 21 (21) (2020).
[21] B. Dunkhunthod, et al., Gymnema inodorum (lour.) Decne. Extract alleviates oxidative stress and inflammatory mediators produced by RAW264.7 macrophages, Oxid. Med. Cell. Longev. 2021 (2021) 8658314.
[22] A. Al-Romaiyan, et al., A novel Gymnema sylvestre extract protects pancreatic beta-cells from cytokine-induced apoptosis, Phytother Res. 34 (1) (2020) 161–172.
[23] K. Shimizu, et al., Structure-activity relationships of triterpenoid derivatives extracted from Gymnema inodorum leaves on glucose absorption, Jpn. J. Pharmacol. 86 (2) (2001) 223–229.
[24] O. Nuchuchua, et al., Relationship of phytochemicals and antioxidant activities in Gymnema inodorum leaf extracts, Heliyon (2023) e23175.
[25] Y.S. Velioglu, et al., Antioxidant activity and total phenolics in selected fruits, vegetables, and grain products, J. Agric. Food Chem. 46 (10) (1998) 4113–4117.
[26] F. Khan, et al., Comprehensive review on phytochemicals, pharmacological and clinical potentials of Gymnema sylvestre, Front. Pharmacol. 10 (2019) 1223.
[27] R.H. Wenger, et al., Frequently asked questions in hypoxia research, Hypoxia 3 (2015) 35–43.
[28] A.V. Kuznetsov, et al., H9c2 and HL-1 cells demonstrate distinct features of energy metabolism, mitochondrial function and sensitivity to hypoxia-reoxygenation, Biochim. Biophys. Acta 1853 (2) (2015) 276–284.
[29] S.C. Bairwa, N. Parajuli, J.R.B. Dyck, The role of AMPK in cardiomyocyte health and survival, Biochim. Biophys. Acta (BBA) - Mol. Basis Dis. 1862 (12) (2016) 2199–2210.
[30] S. Jiang, et al., AMPK: potential therapeutic target for ischemic stroke, Theranostics 8 (16) (2018) 4535–4551.
[31] S. Wu, M.H. Zou, AMPK, mitochondrial function, and cardiovascular disease, Int. J. Mol. Sci. 21 (14) (2020).
[32] D.C. Fuhrmann, B. Brune, Mitochondrial composition and function under the control of hypoxia, Redox Biol. 12 (2017) 208–215.
[33] V.J. Ferrans, W.C. Roberts, Myocardial ultrastructure in acute and chronic hypoxia, Cardiology 56 (1) (1971) 144–160.
[34] G.S. McElroy, N.S. Chandel, Mitochondria control acute and chronic responses to hypoxia, Exp. Cell Res. 356 (2) (2017) 217–222.
[35] D.R. Wise, et al., Hypoxia promotes isocitrate dehydrogenase-dependent carboxylation of alpha-ketoglutarate to citrate to support cell growth and viability, Proc. Natl. Acad. Sci. U. S. A. 108 (49) (2011) 19611–19616.
[36] H.X. Li, et al., Wnt11 preserves mitochondrial membrane potential and protects cardiomyocytes against hypoxia through paracrine signaling, J. Cell. Biochem. 121 (2) (2020) 1144–1155.
[37] M. Serocki, et al., miRNAs regulate the HIF switch during hypoxia: a novel therapeutic target, Angiogenesis 21 (2) (2018) 183–202.
[38] A. Palazon, et al., HIF transcription factors, inflammation, and immunity, Immunity 41 (4) (2014) 518–528.
[39] K. Pham, K. Parikh, E.C. Heinrich, Hypoxia and inflammation: insights from high-altitude physiology, Front. Physiol. 12 (2021) 676782.
[40] K.S. Hewitson, et al., Structural and mechanistic studies on the inhibition of the hypoxia-inducible transcription factor hydroxylases by tricarboxylic acid cycle intermediates, J. Biol. Chem. 282 (5) (2007) 3293–3301.
[41] P. Koivunen, et al., Inhibition of hypoxia-inducible factor (HIF) hydroxylases by citric acid cycle intermediates: POSSIBLE links between cell metabolism and stabilization OF HIF**This work was supported by grants 200471 and 202469 from the health science council and 44843 from the Finnish centre of excellence programme 2000–2005 of the academy of Finland, J. Biol. Chem. 282 (7) (2007) 4524–4532, *the S. Juselius Foundation, and FibroGen Inc. (South San Francisco, CA). The costs of publication of this article were defrayed in part by the payment of page charges. This article must therefore be hereby marked "advertisement" in accordance with 18 U.S.C. Section 1734 solely to indicate this fact*.
[42] P. Hernansanz-Agustín, et al., Acute hypoxia produces a superoxide burst in cells, Free Radic. Biol. Med. 71 (2014) 146–156.
[43] D.C. Fuhrmann, B. Brüne, Mitochondrial composition and function under the control of hypoxia, Redox Biol. 12 (2017) 208–215.
[44] A.K. Knutson, et al., HIF in the heart: development, metabolism, ischemia, and atherosclerosis, J. Clin. Invest. 131 (17) (2021).
[45] J. Schödel, et al., High-resolution genome-wide mapping of HIF-binding sites by ChIP-seq, Blood 117 (23) (2011) e207–e217.
[46] Y. Du, et al., Hypoxia-inducible factor 1 alpha (HIF-1α)/Vascular endothelial growth factor (VEGF) pathway participates in angiogenesis of myocardial infarction in muscone-treated mice: preliminary study, Med. Sci. Mon. Int. Med. J. Exp. Clin. Res. 24 (2018) 8870–8877.
[47] Z. Luo, et al., Hypoxia signaling in human health and diseases: implications and prospects for therapeutics, Signal Transduct. Targeted Ther. 7 (1) (2022) 218.
[48] H. Zhang, N.S. Dhalla, The role of pro-inflammatory cytokines in the pathogenesis of cardiovascular disease, Int. J. Mol. Sci. 25 (2) (2024).
[49] G.W. Dorn, 2nd, Mitochondrial dynamics in heart disease, Biochim. Biophys. Acta 1833 (1) (2013) 233–241.
[50] K. Yamauchi-Takihara, et al., Hypoxic stress induces cardiac myocyte-derived interleukin-6, Circulation 91 (5) (1995) 1520–1524.
[51] M. Sun, et al., Tumor necrosis factor-alpha mediates cardiac remodeling and ventricular dysfunction after pressure overload state, Circulation 115 (11) (2007) 1398–1407.
[52] R. Cauchois, et al., Early IL-1 receptor blockade in severe inflammatory respiratory failure complicating COVID-19, Proc. Natl. Acad. Sci. U. S. A. 117 (32) (2020) 18951–18953.
[53] M.N. Amin, et al., Inflammatory cytokines in the pathogenesis of cardiovascular disease and cancer, SAGE Open Med 8 (2020) 2050312120965752.
[54] S. Ounjaijean, et al., Gymnema inodorum leaf extract improves cardiac function in experimental mice infected with plasmodium berghei, J Evid Based Integr Med 28 (2023), 2515690x221150526.